

Van Andel and G. G. Shor, Jr., Eds. (American Association of Petroleum Geologists Memoir 3, 1964), p. 144; F. F. Wilson, *J. Amer. Ass. Petrol. Geol.* **32**, 1762 (1949).

11. W. Hamilton, *Bull. Geol. Soc. Amer.* **72**, 1307 (1961).
12. E. C. Allison and R. G. Gastil, personal communication.
13. W. R. Normark and J. R. Curray, *Bull. Geol. Soc. Amer.*, in press.
14. N. L. Taliadro, *Calif. Div. Mines Bull.* **118**, 119 (1943).
15. M. L. Hill and T. W. Dibblee, Jr., *Bull. Geol. Soc. Amer.* **64**, 443 (1953).
16. T. E. Chase and H. W. Menard, Topographic charts 3, 4A, 5, and 6 prepared for the U.S. Bureau of Commercial Fisheries (La Jolla, Calif., 1964).
17. The horizontal dimensions of the magnetic block model are taken from Pitman and Heirtzler (19). The top of the model is placed 2.93 km (1640 fathoms) below sea level. It is 1.7 km thick. The blocks are assigned alternating effective susceptibilities of  $\pm 0.01 \text{ emu cm}^{-3}$  oersted<sup>-1</sup> except for the central block which is  $+0.02$ . The blocks were then exposed to the ambient field with the

following characteristics: intensity, 44,000 gammas (1 gamma =  $10^{-5}$  oersted); inclination, 47° down; declination, 10° east. The geomagnetic time scale is taken from Cox *et al.* (8) and Doell and Dalrymple (19).

18. W. C. Pitman III and J. R. Heirtzler, *Science* **154**, 1164 (1966).
19. R. R. Doell and G. B. Dalrymple, *ibid.* **152**, 1060 (1966).
20. Shiptime supported by NSF blockfunding. Research supported by ONR, Marine Physical Lab (SIO), and the U. S. Navy Oceanographic Office. During the past year, detailed magnometer and especially seismic profiling surveys have been conducted up and down the length of the Gulf of California at the same time that we have been carrying out magnometer surveys at the mouth of the Gulf. These geophysical surveys by Moore and Buffington and our work are simultaneous, independent studies that reach similar conclusions based on different bodies of data. All the authors have thus requested publication of both articles at the same time as we believe them to be complementary.

5 April 1968

## Magnetoencephalography: Evidence of Magnetic Fields Produced by Alpha-Rhythm Currents

**Abstract.** *Weak alternating magnetic fields outside the human scalp, produced by alpha-rhythm currents, are demonstrated. Subject and magnetic detector were housed in a multilayer magnetically shielded chamber. Background magnetic noise was reduced by signal-averaging. The fields near the scalp are about  $1 \times 10^{-9}$  gauss (peak to peak). A course distribution shows left-right symmetry for the particular averaging technique used here.*

Fluctuating magnetic fields around the human torso, produced by ion currents from the heart, have been detected (1, 2) and studied (3). I now present evidence for the existence of a much smaller fluctuating magnetic field around the human head; the field is produced by the alpha-rhythm currents commonly seen on the electroencephalogram (EEG). The experiment, with some improvements, was similar to that for detecting the heart's magnetic field (2, 3); a subject with a sensitive magnetic detector near the field source, in this case the head, was situated inside an enclosure which was heavily shielded from external magnetic fluctuations. The high sensitivity of this experiment is due to the use of a low-noise parametric amplifier as part of the detector, and to the effectiveness of the shielding.

In theory, magnetic measurements at or near the surface of a living volume can yield some information about the internal charge distribution not possible to obtain with surface voltage or potential measurements. The potential measurements are limited because in general they cannot uniquely determine an internal charge distribution (4) which, in a living volume, contains the polarized charge layers of excitable muscle

and nerve tissue. In electrocardiography, measurements of surface potential yield information about the state of heart muscles; the anatomical and electrical situations are relatively simple and well-understood, and the accepted electrical model of the heart is adequate for many purposes. As techniques improve, the information extracted with

electrocardiography of any particular heart may soon approach the maximum allowed by this limitation. Because of this, measurements of the heart's magnetic field can eventually serve the auxiliary purpose of reducing this limitation. In electroencephalography, measurements of the brain's magnetic field may have a greater and more direct use. The information extracted by scalp potential measurements (the EEG) is far less than the allowed maximum because of the anatomical, functional, and electrical complexity of the source, for which no simple and effective model yet exists; the complexity is increased by the presence of the skull, a relatively poor conductor. Hence magnetic measurements around the head may supply fundamental information needed simply to evolve an effective electrical model of the phenomena which give rise to the EEG.

In an attempt to detect fluctuating or a-c magnetic fields from the brain, it makes sense to first use the alpha-rhythm currents. On instruction, the subject can produce or remove them by closing or opening his eyes; they yield some of the larger scalp potentials, and they are contained in the relatively narrow frequency band of 8 to 13 hz, with small harmonics; this is important because a narrower detector bandwidth means less detector noise, in which the weak magnetic signal is buried. By using a simplified geometry and formulas developed by Baule (5), one can theoretically predict the alpha-rhythm field several centimeters outside

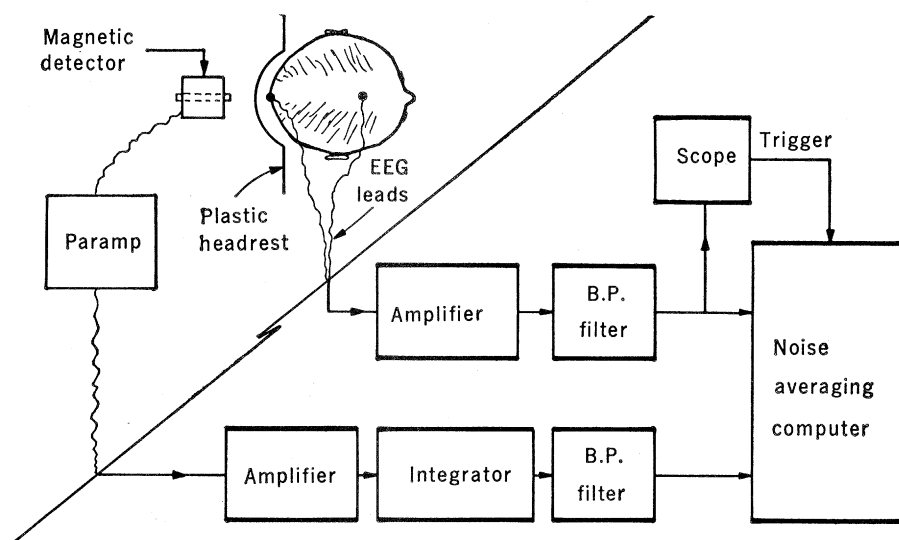


Fig. 1. Arrangement for magnetic alpha-rhythm detection. Subject and detector are inside the shielded enclosure, seen from the top; electronics are at an external station. The ferrite rod on the axis of the electrostatically shielded coil is in line with the subject'sinion; this particular orientation detects the magnetic component normal to the scalp at the back of the head.

Fig. 2. (A and B) MEG noise only after 1000, 4000, and 9000 sweeps; (C)  $4 \times 10^{-10}$  gauss (pp) calibration, with generating current; (D) same but calibration loop flipped; (E-N) upper traces are MEG's, lowers are EEG's; (E) left side of G.B.'s head, normal component, eyes closed; (F) G.B., left side, normal component, eyes open; (G) G.C., left side, normal component, eyes closed; (H) G.C., left side, normal component, eyes open; (I) G.C., right side, normal component, eyes closed; (J) G.C., ferrite removed, left side, normal component, eyes closed; (K) G.C., back of head, horizontal component, eyes closed; (L) F.S., back, normal component, eyes closed; (M) F.S., left side, normal component, eyes closed; (N) F.S., right front, normal component, eyes closed.

the scalp (6) to be  $\sim 7 \times 10^{-10}$  gauss peak to peak (pp), to within an order of magnitude. This is about  $10^{-9}$  of the earth's steady field,  $10^{-5}$  of the earth's fluctuations, and  $10^{-3}$  of the heart's maximum field.

Figure 1 shows the arrangements for detecting this weak field. The enclosure, described in detail elsewhere (7), consists of three nested cubical shells 2 m on the inside; the outer two layers are of moly-permalloy, the inner of welded aluminum. The subject assumed different positions near the fixed detector for different measuring points around the head. The detector was a 1-million-turn (No. 44) coil in a thin-walled, brass electrostatic shield about 9 cm by 9 cm, with a removable ferrite rod core; this distorted the field but increased the flux fourfold. The detector operates because a weak alternating magnetic field induced a small voltage across the coil; this voltage was amplified in several stages, integrated to yield a voltage proportional to magnetic flux, and filtered to a 5-hz bandwidth at 10 hz. The sensitivity was limited by the thermal Johnson noise of the coil, which was greater than both the induced voltage from the magnetic background noise and the parametric amplifier (Texas Instruments RA3) input noise; in the stated bandpass this noise was equivalent to  $\approx 6 \times 10^{-9}$  gauss (root-mean-square). The expected signal was then  $\approx 0.03$  of the noise, and a computer of average transients (CAT) was used to extract the signal from the noise.

Each sweep of the CAT was triggered at a chosen phase of the EEG obtained from the precentral region and inion, and filtered to almost match the magnetic bandpass; perfect matching was difficult because of coil resonance at 35 hz. The EEG signal was stored

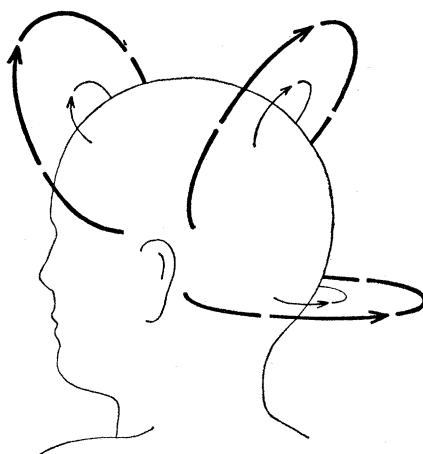
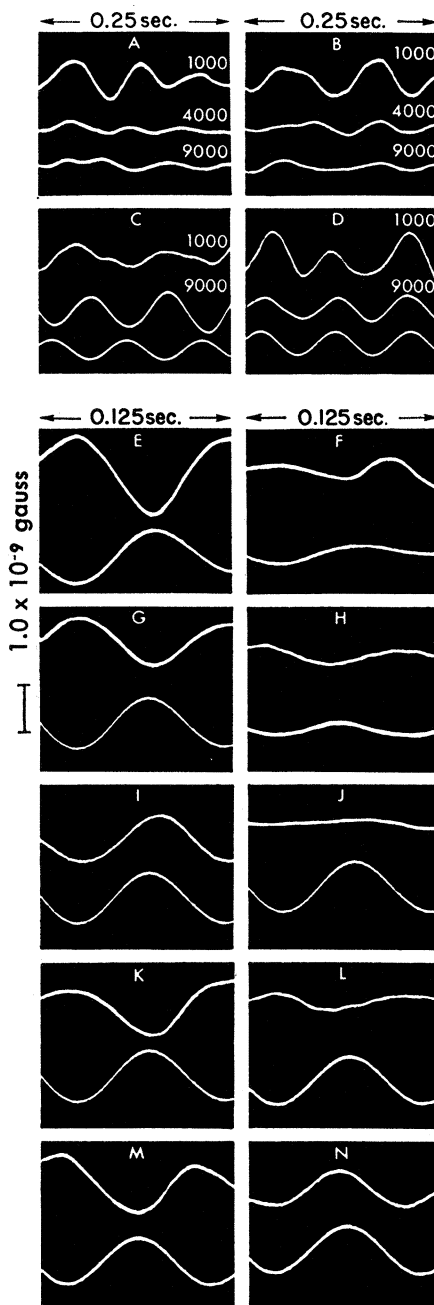


Fig. 3. General features of the measured B-vector distribution around the head due to alpha-rhythm currents, inion-trigger averaging being used.

separately but simultaneously with the magnetoencephalogram (MEG). The system was therefore designed to search for an MEG produced only in coincidence with the EEG sampled from two particular scalp points.

Four subjects with alphas above average were chosen. Measurements on all four consistently showed the presence of an MEG signal, with a maximum of  $\approx 1 \times 10^{-9}$  gauss (pp). To within the coarseness of the experimental sampling, the MEG's varied similarly around the four scalps.

Figure 2 contains calibrations and results. The scale refers to all MEG's. (A) and (B) are MEG's from two different runs, a trigger from a 10-hz oscillator being used instead of the EEG; therefore the MEG's are only random thermal noise which decreases as the square root of the number of sweeps. Since the expected fields are  $> 3 \times 10^{-10}$  gauss (pp), I decided to use 2500 sweeps in most runs, including (E) to (N); these took about 8 minutes. (C) and (D) are MEG calibrations with a 10-hz alternating field from a nearby current loop, also showing the current wave current; the signal is well-extracted out of the noise after 9000 sweeps. The loop was flipped over for (D) as a standard check; except for some noise, the phase reverses by  $180^\circ$ . (E) and (F) are typical MEG's obtained when the eyes are opened or closed, as are (G) and (H). When the eyes were closed, an MEG signal was coincident with the EEG, at about four times the noise level for 2500 sweeps; when the eyes were open both the MEG and EEG signals dropped appropriately. (I) shows the phase reversal at the other side of the head; this was seen on all subjects. Removal of the ferrite (J) drops the trace into the noise level, verifying the signal's magnetic origin; (K) and (L) show the B-vector orientation at the back of the head to be parallel to the scalp, since there is no significant normal component. (M) is similar to (E) on another subject; (N) shows the signal at the right temple.

Lengthy auxiliary experiments were performed to verify that the signal in, for example, Fig. 2E was due to alpha-rhythm currents and no other source. Each phenomenon which seemed capable of falsely producing the same results was repeatedly and systematically ruled out. Some of these are: the heart's magnetic field at the head, feedback from the external EEG amplifier to the

magnetic detector, and magnetic noise which induces both a detector and an EEG voltage. Curious phenomena were indeed occasionally seen, but these were eventually understood and avoided. For example, poor contacts between EEG leads and the scalp resulted in 60-hz pickup in the EEG line which influenced the triggers with eyes open, thereby selecting 60 hz magnetic subharmonics near 10 hz to stand out on the MEG.

Figure 3 shows the course B-vector distribution at an arbitrary phase of the alpha cycle, averaged over 2500 cycles. The distribution remains the same if the upper EEG lead is moved to another point, at about the same alpha-rhythm potential, say the right ear. No measurements have yet been made with the inion lead moved, but one would expect a different distribution. Such measurements with resulting magnetic distributions would probably reveal information about the internal alpha-rhythm sources, and would be a first step in evaluating the possible uses of the MEG.

DAVID COHEN

Department of Physics,  
University of Illinois at Chicago Circle,  
Chicago 60680

#### References and Notes

1. G. M. Baule and R. McFee, *Amer. Heart J.* **66**, 95 (1963).
2. D. Cohen, *Science* **156**, 653 (1967).
3. A paper with results of extensive magneto-cardiographic mapping of ten human heart subjects has been submitted for publication.
4. For example, potential measurements on a spherical surface which contains a concentric, radially pulsating shell of charge cannot yield the instantaneous charge radius. In this case, magnetic measurements on the surface are always zero and of no help. A case illustrating magnetic use is an irregular, closed volume containing three irregular, successively enclosed regions. The inner region is conducting and contains currents and their sources; the middle region is insulating and nonreactive; and the outer region is conducting. The outer surface potential will be instantaneously constant and hence reveal nothing about the inner source distribution, but the surface magnetic measurements will show internal currents, hence some information about the source distribution.
5. G. Baule and R. McFee, *J. Appl. Phys.* **36**, 2066 (1965).
6. I assume the head to be approximated by an alternating electric dipole inside and parallel to the surface of a semi-infinite volume conductor of 1000 ohm-cm resistivity. The dipole makes an a-c distribution within the medium which produces an external alternating magnetic field, the maximum of which depends only on the maximum surface potential. I chose 30 $\mu$ v (pp) as that part of the voltage not due to a perpendicular dipole, which contributes zero external magnetic field.
7. D. Cohen, *J. Appl. Phys. Suppl.* **38**, 1296 (1967).
8. I thank Prof. H. Fernandez-Moran, Prof. F. Gibbs, and Prof. J. Hughes for their help and encouragement. Supported by the Research Corporation.

11 June 1968

group could not be assigned because of twinning noted in the patterns. Hence, the true *a* and *c* axes may differ from those given. The cell chosen is, however, allowable and is the one consistent with morphological examination. The powder diffraction pattern (Table 2) was not indexed because of the large size of the cell which leads to too many ambiguities and multiple index assignments.

Krinovite is deep emerald green. In sodium light  $\alpha = 1.712 \pm 0.002$ ;  $\beta$ ,  $1.725 \pm 0.002$ ;  $\gamma$ ,  $1.760 \pm 0.005$ ; bi-axial +; and  $2V$ ,  $61^\circ \pm 2^\circ$ , measured, and  $64^\circ$ , calculated. The optic axial plane is parallel to *b*. Pleochroism is intense, *X* (= *b*) is yellow-green; *Y*, blue-green; and *Z*, greenish black (sometimes an anomalous dark reddish brown). Dispersion of the refractive indices is strong, but no optic axis dispersion could be detected. No cleavage was observed. Most grains showed multiple twinning.

The hardness is between 5.5 and 7. Density was determined by the sink-or-float method as 3.38 g/cm<sup>3</sup>; the calculated x-ray density is 3.44 g/cm<sup>3</sup> based on *Z* = 32.

Approximately 50 unsuccessful attempts were made to synthesize krinovite. Mixtures of Cr<sub>2</sub>O<sub>3</sub>, Na<sub>2</sub>SiO<sub>3</sub>, SiO<sub>2</sub>, and MgO heated in air in platinum for several days to several weeks at 700° to 1400°C invariably resulted in considerable oxidation of chromium with the formation of some sodium chromate. In some cases magnesiochromite was formed. Ureyite, NaCr(SiO<sub>3</sub>)<sub>2</sub> (5), was readily formed. Similar attempts in an argon atmosphere or in vacuum, in both platinum and graphite crucibles, resulted in the formation of gray-green enamels within which spinel and unidentifiable phases were dispersed. Attempts at 25 kb and 650° to 1400°C were unsuccessful.

Natural krinovite heated in air at 1000°C for 10 days lost its green color. Olivine was the only phase that could be identified among the decomposition products. Ureyite, similarly treated, was virtually unaffected. Natural krinovite was also heated in vacuum for 6 days at 1000°C and again lost its color. Decomposition products were magnesiochromite, cristobalite, and unidentifiable phases. We must conclude that temperatures in the whole range examined (650° to 1400°C) are probably too high for the stable, or metastable, formation of krinovite.

The dominant associated minerals in both Canyon Diablo and Wichita

## Krinovite, NaMg<sub>2</sub>CrSi<sub>3</sub>O<sub>10</sub>: A New Meteorite Mineral

**Abstract.** *An unusual new silicate, krinovite, has been discovered within graphite nodules in three iron meteorites. Its ratio of silicon to oxygen of 3 : 10 suggests a rare kind of silicate polymerization. The meteorite nodules in which it occurs exhibit a chemical fractionation that differs from that of both stone meteorites and terrestrial basalt.*

Krinovite (kreen'-off-ite), a mineral unknown in any terrestrial rock, occurs as minute subhedral grains (largest approximately 200  $\mu$ ) disseminated within graphite nodules in the octahedrite iron meteorites Canyon Diablo (United States), Wichita County (United States), and Youndegin (Australia).

The composition (Table 1) was determined by electron microprobe methods (1), and the observed variations are given in the table. The simplified empirical formula is NaMg<sub>2</sub>CrSi<sub>3</sub>O<sub>10</sub>. The 3 : 10 ratio of silicon to oxygen suggests a very unusual silicate polymerization into short chains, each consisting of three tetrahedral units in which two oxygens are shared. This type of polymerization has recently been encountered by Donnay and Allmann (2) in the rare terrestrial mineral ardennite, in which both Si<sub>3</sub>O<sub>10</sub> and single tetrahedral SiO<sub>4</sub> units occur. More recently

Moore and Bennett (3) established the presence of these same polymerized units, partially aluminous, (Al,Si)<sub>2</sub>SiO<sub>10</sub>, in the structure of the rare mineral kornerupine. In this mineral the units occur with the double-linked tetrahedral pairs Si<sub>2</sub>O<sub>7</sub>. Krinovite may be the first example of a mineral with purely Si<sub>3</sub>O<sub>10</sub> units. On the other hand, it must be noted that the empirical formula could be written in other ways which suggest mixed polymerizations in well-known ratios: NaMg<sub>2</sub>Cr(SiO<sub>4</sub>)(SiO<sub>3</sub>)<sub>2</sub> or NaMg<sub>2</sub>Cr(Si<sub>2</sub>O<sub>7</sub>)(SiO<sub>3</sub>). By multiplying the "molecule" by integers 2, 3, and so forth, other combinations are possible.

Single-crystal measurements (Weissenberg camera) indicate monoclinic symmetry with *a* =  $19.48 \pm 0.04$  Å; *b*,  $29.18 \pm 0.06$  Å; *c*,  $10.25 \pm 0.02$  Å, and  $\beta$ ,  $103^\circ \pm 2^\circ$  (4). The cell dimensions given here are observed in the single-crystal pattern; however, a space